Thermochimica Acta 512 (2011) 67–70

Contents lists available at ScienceDirect

Thermochimica Acta

journal homepage: www.elsevier.com/locate/tca

Kinetics of nonisothermal crystallization of Cs_2O–Fe_2O_3–P_2O_5 glasses

Kitheri Joseph, R. Venkata Krishnan, K.V. Govindan Kutty*, P.R. Vasudeva Rao

Chemistry Group, Indira Gandhi Centre for Atomic Research, Kalpakkam, Tamil Nadu, India

ARTICLE INFO

Article history:
Received 30 June 2010
Received in revised form 31 August 2010
Accepted 1 September 2010
Available online 15 September 2010

Keywords:
Crystallization kinetics
Differential scanning calorimetry
Nonisothermal
Isoconversional
Activation energy

ABSTRACT

The crystallization kinetics of Cs_2O–Fe_2O_3–P_2O_5 glasses containing 12.5–27 mol% Cs_2O were studied by using differential scanning calorimetry under nonisothermal conditions. Strong dependence of activation energy with temperature was observed, indicating the complex nature of the crystallization process. The various crystallization products were identified by X-ray diffraction technique. $CsFeP_2O_7$ was found to be the major crystalline phase in all cases. The overall activation energy obtained by classical model-free kinetic method was compared with that of isoconversional method; and from the results, the dependence of activation energy on extent of reaction and average temperature was delineated.

1. Introduction

Iron phosphate glasses (IPG) are considered as potential host matrices for the immobilization of high level waste (HLW) [1,2]. Among the various constituents of HLW, a large amount of thermal energy is produced during the radioactive decay of ^{137}Cs and ^{90}Sr. It is advantageous to separate Cs and Sr and immobilize in a suitable matrix [3]. The thermal energy associated with radioactive decay can even crystallize the glasses when loaded with excessive amounts of ^{137}Cs or ^{90}Sr. This can be simulated by studying the thermal crystallization of glasses containing Cs and Sr. In our previous work [4], the crystallization behaviour of iron phosphate glass loaded with 36 mol% Cs_2O was studied by differential scanning calorimetry (DSC) technique. The present work is on the crystallization and evaluation of activation energy of crystallization of 12.5–27 mol% of Cs_2O loaded iron phosphate glasses. The experiments were carried out by using DSC under nonisothermal conditions. The activation energy was determined by the classical model-free kinetic method as well as by the isoconversional method.

2. Experimental

The Cs_2O–Fe_2O_3–P_2O_5 glasses with varying Cs_2O content were prepared by the conventional melt-quench technique. The preparation conditions and compositional analysis along with the thermal and Mossbauer characterization are explained in detail elsewhere [5]. The glasses under present study are referred to as IP8C2, IP7C3 and IP6C4 whose nominal compositions are presented in Table 1.

DSC (M/s. Mettler Toledo model DSC 821e/700) was employed to understand the crystallization behaviour of cesium loaded iron phosphate glasses under flowing argon at a flow of 50 ml/min. The DSC equipment was calibrated for temperature as explained in Ref. [6]; the accuracy of temperature measurement was ±1 K. The DSC experiments were performed at various heating rates (2, 5, 7, 10 and 15 K/min) using 7 mg of glass powder in a Pt crucible. The variation in the amount of sample used for crystallization studies was within ±2 μg.

The products of crystallization were characterized by XRD technique (Siemens D500 X-ray diffractometer employing Cu Kα radiation). The IP6C4 glass was annealed at 878 K in flowing Ar atmosphere for 30 min. IP7C3 and IP8C2 glasses were annealed at two different temperatures namely 853 K (for 10 min) and 913 K (for 30 min) and the crystallized products were identified by XRD. The annealing temperature was chosen based on the DSC results which showed single crystallization curve for IP6C4 and two for IP7C3 and IP8C2.

3. Results and discussion

3.1. Characterization of crystallized products

The XRD pattern of the annealed (878 K) IP6C4 glass is shown in Fig. 1. The XRD pattern of the annealed specimen shows the diffraction lines corresponding to $CsFeP_2O_7$, $Cs_3Fe_4(PO_4)_5$ and Cs_3PO_4, the major phase being $CsFeP_2O_7$. The major lines present in the XRD

* Corresponding author. Fax: +91 44 2748 0065.
E-mail address: kvg@igcar.gov.in (K.V. Govindan Kutty).

0040-6031/$ – see front matter © 2010 Published by Elsevier B.V.
doi:10.1016/j.tca.2010.09.001

Table 1
Nominal composition of the glasses as determined by XRF technique [5].

Sample code	Glass composition (mol%)		
	Fe_2O_3	P_2O_5	Cs_2O
IP8C2	34.5	53	12.5
IP7C3	33	46	21
IP6C4	29	44	27

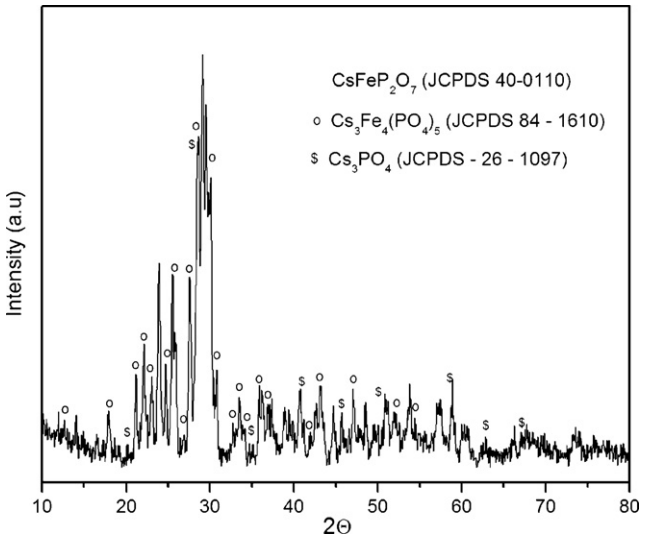

Fig. 1. XRD pattern of the IP6C4 glass annealed at 878 K.

pattern of the annealed IP7C3 glass (Fig. 2) at 853 and 913 K were found to be similar. The pattern corresponding to 853 K shows the presence of an amorphous phase coexisting with the crystalline phase. The X-ray pattern at 853 K clearly shows the formation of crystalline $CsFeP_2O_7$ and the minor phases could not be ascertained due to very low intensity. The annealed sample is crystalline at 913 K and the XRD pattern indicates that the IP7C3 glass crystallizes to a mixture of $CsFeP_2O_7$, $FePO_4$ and Fe_2O_3. Similarly, the IP8C2 also shows the crystalline phase coexisting with an amorphous phase at 853 K. At 913 K, the IP8C2 glass crystallizes to a mixture of $CsFeP_2O_7$, $Fe(PO_3)_3$ and Fe_2O_3 as shown in Fig. 3. $CsFeP_2O_7$ phase was found to be the major phase in all the three ternary cesium loaded iron

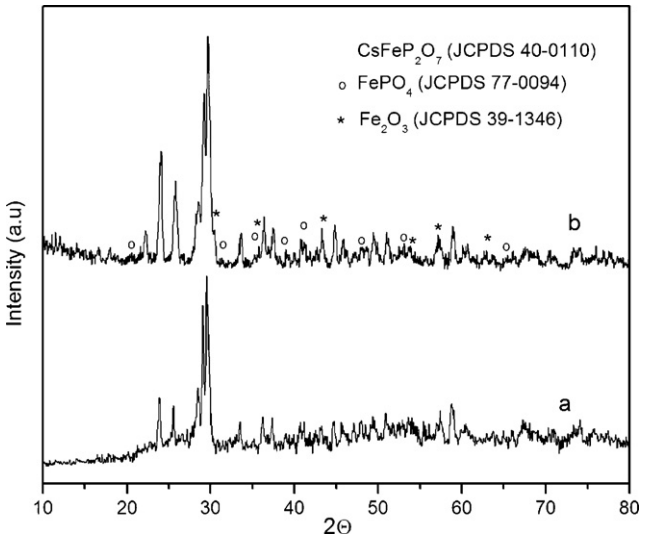

Fig. 2. XRD pattern of the crystallized products of IP7C3 glass at (a) 853 K and (b) 913 K.

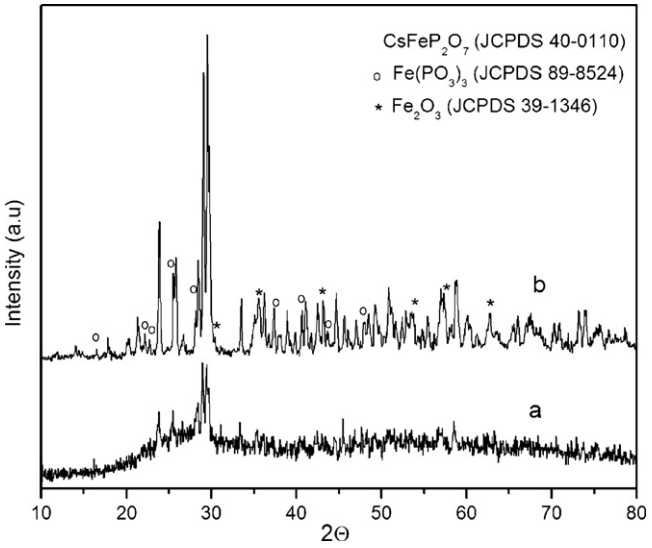

Fig. 3. X-ray diffraction pattern of IP8C2 glass crystallized at (a) 853 K and (b) 913 K.

phosphate glasses under study, indicating pyrophosphate type of linkage in the glass. The minor phases varied depending on the composition of the glass. The pyrophosphate linkage was confirmed in all the cesium iron phosphate glasses by our earlier study on the glass structure by infrared spectroscopy [7]. Similar pyrophosphate linkage was also found in various ternary alkali phosphate glasses [8,9]. But, binary iron phosphate glasses were known to crystallize to various products like $FePO_4$, $Fe(PO_3)_3$, $Fe(PO_3)_2$, $Fe_4(P_2O_7)_3$, $Fe_7(PO_4)_6$, $Fe_3(P_2O_7)_2$, $Fe_3(PO_4)_2$, Fe_2O_3 and FeO depending on the composition and the Fe^{2+}/Fe^{3+} ratio [10–15]. The iron based glasses richer in Fe^{2+} content crystallize to ferrous metaphosphate ($Fe(PO_3)_2$), ferrous-ferric pyrophosphate ($Fe_3(P_2O_7)_2$) and ferrous-ferric orthophosphate ($Fe_7(PO_4)_6$), whereas the iron phosphate glasses richer in Fe^{3+} content crystallize to ferric orthophosphate ($FePO_4$), ferric metaphosphate ($Fe(PO_3)_3$) and ferric pyrophosphate ($Fe_4(P_2O_7)_3$). The glasses under the present study were very rich in Fe^{3+} content (95–98%) [5], and thus the crystallization products were ferric phosphates (pyro, meta or ortho) instead of ferrous phosphates.

3.2. Kinetic analysis

DSC experiments were carried out on the IP6C4 glass at various heating rates in the temperature range of 825–975 K as shown in Fig. 4. The onset of crystallization temperature was found to vary linearly with heating rate. A single exothermic peak was obtained for all heating rates and as expected the exothermic peak shifted to higher temperatures with increasing heating rate [16]. The apparent crystallization temperature was obtained by extrapolating the linear fit to zero heating rate and the value obtained is 859 K (insert in Fig. 4). The crystallization kinetics can be described by the following general expression assuming Arrhenius type temperature dependence of rate constant [17] as,

$$\frac{d\alpha}{dt} = Ae^{-(E_a/RT)}f(\alpha) \quad (1)$$

where t is the time, T the absolute temperature; α the fraction crystallized; A the pre-exponential factor; E_a the activation energy of crystallization, and R, the gas constant. The $f(\alpha)$ is the reaction model. Under nonisothermal conditions with a fixed heating rate β, Eq. (1) can be rewritten as [17]:

$$\frac{d\alpha}{dT} = \frac{A}{\beta}e^{-(E_a/RT)}f(\alpha) \quad (2)$$

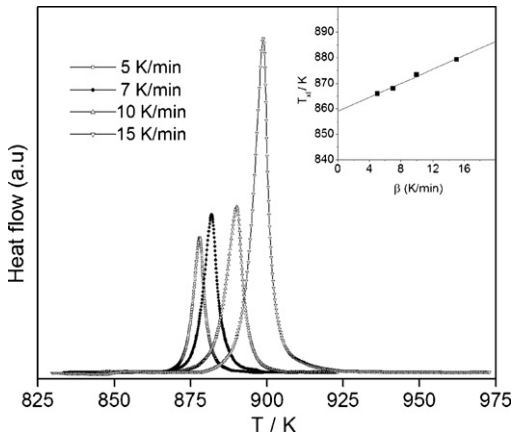

Fig. 4. DSC traces for IP6C4 glass at various heating rates. Crystallization temperature as a function of heating rate is shown as an insert; solid line shows the linear fit.

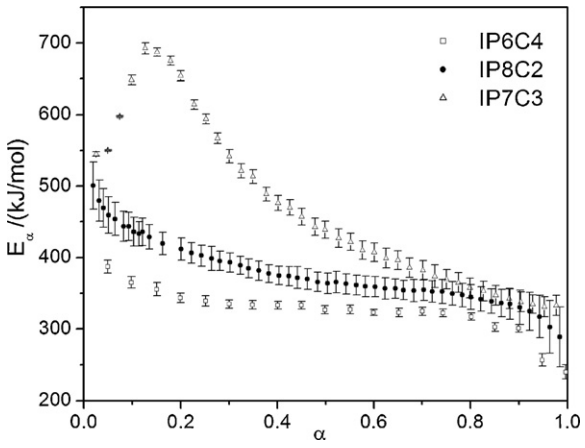

Fig. 5. Plot of E_α and as a function of fraction crystallized (α) for the IP6C4, IP7C3 and IP8C2 glasses.

The above equation can be solved to evaluate activation energy by classical Kissinger method [17], which assumes the maximum reaction rate at the peak temperature (T_p). The activation energy can be obtained by using the following equation:

$$\ln \frac{\beta}{T^2} = \text{const} - \frac{E_a}{RT_p} \quad (3)$$

A plot of $\ln(\beta/T^2)$ vs $1/T_p$ gives a straight line with the slope $(-E_a/R)$, from which the activation energy can be evaluated. The activation energy obtained by Kissinger method is 318 ± 29 kJ/mol. Though the overall activation energy for the crystallization of glass can be obtained by Kissinger method, model-free isoconversional method [18] is more reliable for understanding the crystallization behaviour and the trend in the activation energy as a function of fraction of crystallization. The evaluation of activation energy by isoconversional method is carried out as discussed below.

The fraction crystallized, α, was evaluated from the DSC curve as a function of temperature at various heating rates. The α vs T curve was found to be sigmoidal in nature. The Kissinger–Akahir–Sunose (KAS) method [19,20] of isoconversion was applied to the crystallization; this takes the form:

$$\ln \frac{\beta_i}{T_{\alpha,i}^2} = \text{const} - \frac{E_\alpha}{RT_{\alpha,i}} \quad (4)$$

where the subscript 'i' denotes the various heating rates. The slope of the plot $\ln \beta_i/T_{\alpha,i}^2$ vs $1/T_{\alpha,i}$ gives the value of effective activation energy, E_α. The plot of E_α as a function of α, the fraction crystallized is shown in Fig. 5. The plot shows the continuous decrease of activation energy with α. The dependence of average temperature (evaluation of average temperature is described in Ref. [4]) is also shown in Fig. 6. This plot clearly indicates that the activation energy decreases with the temperature. This type of behaviour [21] cannot be explained by a single step mechanism, but by a complex mechanism involving two processes namely, nucleation and diffusion. The activation energy for these two processes can be different and hence the effective activation energy [22] varies with α and temperature as observed in Figs. 5 and 6.

Similar crystallization experiments were carried out for the glasses IP7C3 and IP8C2. The crystallization of IP7C3 and IP8C2 appears as two exothermic peaks. Fig. 7 shows a typical DSC curve of IP7C3 and IP8C2 at 10 K/min along with IP6C4. From the DSC curves of IP7C3 and IP8C2 as a function of temperature with varying heating rates, the apparent crystallization temperature was evaluated. The crystallization temperature was found to vary linearly with heating rate. The first and second crystallization of IP7C3 occurs at 864 and 879 K respectively, whereas that of IP8C2 is 870 and 897 K

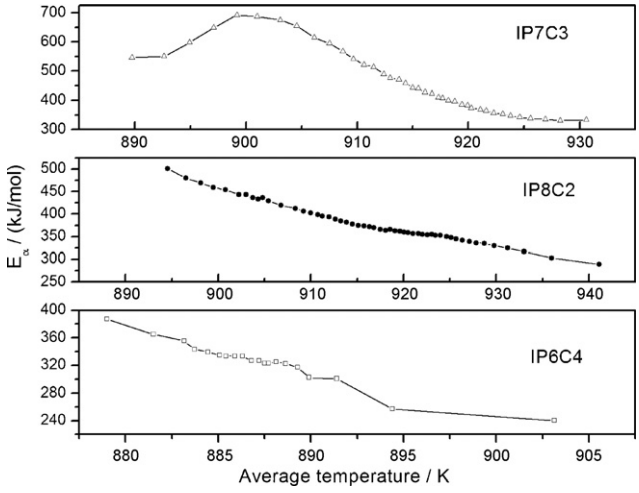

Fig. 6. Plot of E_α and as a function of average temperature for the IP6C4, IP7C3 and IP8C2 glasses.

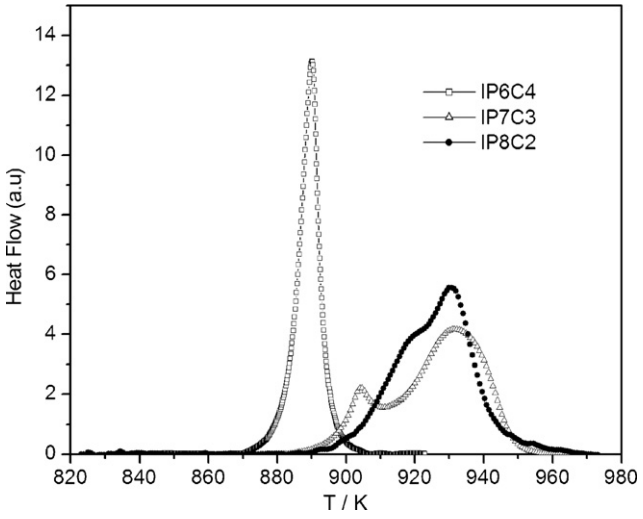

Fig. 7. Typical DSC curves for the crystallization of IP6C4, IP7C3 and IP8C2 glasses in argon at 10 K/min.

respectively. Comparing the crystallization temperature of IP6C4, IP7C3 and IP8C2, it is clear that the crystallization temperature decreases as the cesium content increases as seen from Fig. 7.

Dependence of fraction of crystallization as a function of temperature at various heating rates was evaluated for IP7C3 and IP8C2 glasses. The activation energy of crystallization process was obtained by the Kissinger method. The activation energies obtained for the first and second crystallization of IP7C3 are 384 ± 26 and 393 ± 64 kJ/mol, whereas those of IP8C2 are 417 ± 6 and 371 ± 9 kJ/mol respectively. The activation energy based on Kissinger method of evaluation for the crystallization of binary IPG was reported in Ref. [23] and the values for the first and second crystallization peaks are 325 ± 10 and 365 ± 10 kJ/mol respectively. By comparing the first crystallization of IP7C3 and IP8C2 with single crystallization of IP6C4, it is clear that the activation energy (by Kissinger method) obtained for the cesium loaded IPG glasses show a decreasing trend with increasing cesium content. Though the activation energy for the first crystallization shows a decreasing trend with increasing cesium content, the activation energy obtained for the second crystallization is found to be marginally higher for IP7C3 compared to that of IP8C2. In our earlier studies [5], during the evaluation of glass transition temperature, IP7C3 glass (21 mol% Cs_2O) was found to have higher glass transition temperature compared to IP8C2 (12.5 mol% Cs_2O), IP6C4 (27 mol% Cs_2O) and the 36 mol% Cs_2O loaded IPG indicating a higher stability of IP7C3 glass. This observed fact could not be explained unambiguously by the trend obtained in the activation energy determined by Kissinger method.

By applying KAS isoconversional method, the dependence of activation energy on the fraction crystallized of IP8C2 glass was determined and represented in Fig. 5. Though two exothermic peaks were found during crystallization of the IP8C2 glass, the dependence of activation energy with α was similar to that of IP6C4. The activation energy decreases with average temperature (Fig. 6) indicating, the complex nucleation–diffusion mechanism during the crystallization of IP8C2.

The dependence of activation energy on α for the crystallization of IP7C3 is also shown in Fig. 5. The dependence of E_α on α for IP7C3 is found to be different from that of IP8C2 and IP6C4. The E_α value increases up to the value of $\alpha = 0.12$ and then decreases continuously with α. The dependence of E_α with average temperature is shown in Fig. 6, which also shows the same trend. During the initial crystallization period, i.e., up to $\alpha = 0.12$, an increase in activation energy is observed. Generally, the increase in E_α with α corresponds to parallel reaction [24]. Beyond the α value of 0.12, the activation energy decreases with α, as observed during the crystallization of IP6C4 and IP8C2. Thus, the crystallization of IP7C3 involves a complex mechanism of parallel reaction followed by a nucleation and diffusion mechanism as the reaction progresses. The isoconversional analysis clearly shows the increase in activation energy during initial crystallization and the value of activation energy (maximum value of 692 kJ/mol) is also higher for the crystallization of IP7C3 (21 mol% Cs_2O) glass. At a fixed α, the activation energy evaluated (isoconversional method) for the IP8C2 and IP6C4 are always lower than that of IP7C3 as seen from Fig. 5. The larger activation energy of IP7C3 indicates higher resistance to crystallization. Thus, isoconversional method explains the better stability of IP7C3, which could not be brought out by the classical model-free method of kinetic analysis.

4. Conclusion

The crystallization kinetics of three cesium iron phosphate glasses were studied by DSC under nonisothermal conditions. $CsFeP_2O_7$ is found to be the major phase present in all the crystallized products as observed by XRD. The activation energy was evaluated by classical model-free kinetic method and by isoconversional methods. The better thermal stability of the IP7C3 glass could not be explained by classical Kissinger method, whereas, the isoconversional method clearly delineate the change in the effective activation energy with α and the average temperature and explains the better stability of the IP7C3 glass.

Acknowledgement

The authors thank Shri. R. Asuvathraman for his kind and continuous help during the calculation of kinetic parameters. The authors also thank Dr. K. Nagarajan for his support during DSC runs.

References

[1] D.E. Day, Z. Wu, C.S. Ray, P. Hrma, J. Non-Cryst. Solids 241 (1998) 1.
[2] M.G. Mesko, D.E. Day, J. Nucl. Mater. 273 (1999) 27.
[3] M.G. Mesko, D.E. Day, B.C. Bunker, Waste Manage. 20 (2000) 271.
[4] K. Joseph, R. Venkata Krishnan, K.V. Govindan Kutty, P.R. Vasudeva Rao, Thermochim. Acta 494 (2009) 110.
[5] K. Joseph, K.V. Govindan Kutty, P. Chandramohan, P.R. Vasudeva Rao, J. Nucl. Mater. 384 (2009) 262.
[6] R. Venkata Krishnan, K. Nagarajan, Thermochim. Acta 440 (2006) 141.
[7] K. Joseph, M. Premila, S. Thomas, G. Amarendra, K.V. Govindan Kutty, C.S. Sundar, P.R. Vasudeva Rao, Materials Chemistry and Physics (communicated).
[8] X. Fang, C.S. Ray, D.E. Day, J. Non-Cryst. Solids 319 (2003) 314.
[9] J. Pan, J. Gong, Key Eng. Mater. 336–338 (2007) 1827.
[10] D.E. Day, C.S. Ray, K. Marasinghe, M. Karabulut, X. Fang, DOE Report 55110, http://www.osti.gov/em52/final_reports/55110.pdf.
[11] A. Mogus-Milankovic, D.E. Day, K. Furic, Key Eng. Mater. 132–136 (1997) 2212.
[12] C.S. Ray, X. Fang, M. Karabulut, G.K. Marasinghe, D.E. Day, J. Non-Cryst. Solids 249 (1999) 1.
[13] J. Doupovec, J. Sitek, J. Kákoš, J. Therm. Anal. 22 (1981) 213.
[14] F.J.M. Almeida, J.R. Martinelli, C.S.M. Partiti, J. Non-Cryst. Solids 353 (2007) 4783.
[15] D.O. Russo, D.S. Rodrıguez, J. Ma, L. Rincon, M. Romero, C.J.R. Gonzalez Oliver, J. Non-Cryst. Solids 354 (2008) 1541.
[16] A.F. Kozmidis-Petrovic, G.R. Strbac, D.D. Strbac, J. Non-Cryst. Solids 353 (2007) 2014.
[17] M.E. Brown, D. Dollimore, A.K. Galwey, Comprehensive Chemical Kinetics, vol. 22, Elsevier, Amsterdam, 1988, p. 99.
[18] N. Sbirrazzuoli, S. Vyazovkin, Thermochim. Acta 388 (2002) 289.
[19] A.A. Abu-Sehly, Thermochim. Acta 485 (2009) 14.
[20] A.A. Joraid, Thermochim. Acta 456 (2007) 1.
[21] A.A. Abu-Sehly, A.A. Elabbar, Physica B 390 (2007) 196.
[22] S. Vyazovkin, I. Dranca, Macromol. Chem. Phys. 207 (2006) 20.
[23] D.E. Day, C.S. Ray, K. Marasinghe, First Year Technical Report, Project no. DE FG07 96ER45618, 1997.
[24] S. Vyazovkin, A.I. Lesnikovich, Thermochim. Acta 165 (1990) 273.